N-enriched GO Adsorbent Series for Selective Adsorption of CO_2: Characterization, Equilibrium, and Thermodynamic Studies

Mahsa Najafi[1], Yasamin Hosseini[2], Soodabeh Khalili[3,*], Mohsen Jahanshahi[3], Majid Peyravi[3]

[1] Department of Chemical Engineering, Faculty of Engineering, University of Tehran, Iran

[2] School of Chemical Engineering, Kavosh Institute of Higher Education, Mahmood Abad, Iran

[3] Nanotechnology Research Institute, Department of Chemical Engineering, Babol Noshirvani University of Technology, Babol, Iran

*Corresponding author Address:

Department of Chemical Engineering, Babol Noshirvani University of Technology, Shariati Av., Babol, P.O. Box: 484, 47148-71167, Iran

Tel/Fax: +98 1132320342

Email: soodabeh.khalili@yahoo.com

GRAPHICAL ABSTRACT

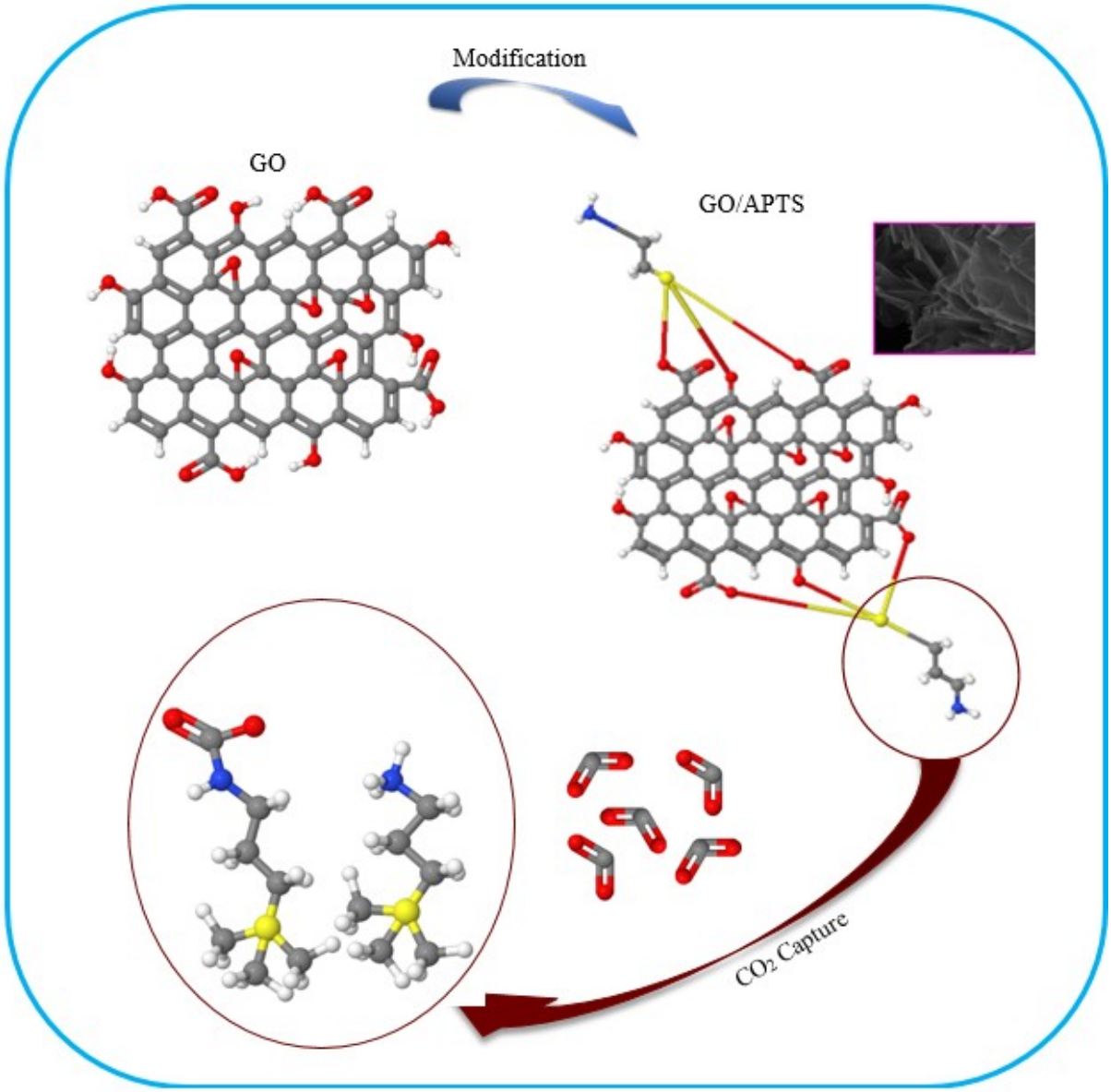

24

ABSTRACT:

In this study a series of GO-based adsorbents were assembled via impregnation method using N-resources: 3-aminopropyl-triethoxysilane (APTS) as primary amio-silane, Piperazine (PIP) as secondary cyclic diamine, and ethanolamine (EA) as primary amine. The influence of amine type, adsorption temperature and pressure were undertaken to obtain the best CO_2 adsorption performance. The characterizing techniques including FTIR, SEM, TGA, BET, BJH, and MP confirmed well impregnation of amine functionalities to the GO framework and high thermal stability of adsorbents. GO/APTS showed the maximum CO_2 uptake (43.114 mmol/g) predicted by the Sips isotherm model and the highest CO_2 (15% V, balanced N_2) selectivity (33.7 %) estimated by the ideal adsorbed solution theory. The experimental adsorption capacity of GO/APTS is 2.3 times higher than pristine GO. This behavior highlights the role of electron-donor amine and methyl groups and high molecular weight of APTS as well as high interfacial area of GO/APTS in CO_2 capture.

KEYWORDS: CO_2 Capture, Amine, Functionalization, Porous Adsorbent.

1. INTRODUCTION

The intensive human activities result in the fast-increasing emission of atmospheric CO_2 [1]. CO_2 is recognized as the prime cause of global warming and literature surveys showed the 60% correspondence of global warming to the emission of CO_2 [2–4]. Based on the fifth report of Intergovernmental Panel on Climate Change (IPCC), the increment of CO_2 emissions brings about strict global warming with severe climate consequences [5]. Therefore, serious strategies for the decrement of CO_2 emissions should be considered. In this context, the exclusion of CO_2 from flue gases is highly considered for mitigation and control of air pollution as well as global warming [6]. Among the multitudinous technologies invented for the capture of CO_2, absorption by liquid alkanol amine solution has received extensive consideration due to its advantages such as high CO_2 selectivity or regeneration of formed carbamates during the process. Despite these advantages, high expenditure of energy for recovery of solvent, intense corrosivity of alkanol amine solvent, along with the oxidation of solvent hider its further commercial applications [7–9]. In this regard, scholars try to find techniques that would respond to deficiencies of absorption by aqueous amine. In search for an appropriate method, amine-functionalized solid adsorbents have revealed a promising potential for the capture of CO_2 [10–12]. The amine-loaded adsorbents have attracted researchers because of their inexpensive, less corrosivity, high stability, and low energy consumption for recovery of adsorbents in comparison with liquid amine absorbing techniques [13–15]. Hence, diverse types of solid adsorbents have been examined for their effectiveness for CO_2 capture. Metal-organic frameworks (MOFs) [16,17], and carbon-based materials [18,19] are among pioneering porous solid adsorbents for the capture of CO_2. Various carbonaceous adsorbents in the forms of for example molecular sieve, nanotube, and fiber have emerged as prospective CO_2 capturing materials for their chemical and thermal merits [20].

63 Graphene is a cheap allotrope of carbon with a high specific surface area which makes it a
64 favorable nexus of CO_2 capture adsorbents [21].
65 Graphene oxide (GO) is a fascinating carbonaceous material [22] that is fabricated from the
66 oxidation of graphite and contains numerous oxygen functionalities such as epoxide, hydroxyl,
67 carboxyl functionalities on its frameworks and borders [23,24]. These functional groups donor
68 GO a striking potential of functionalization via covalent and non-covalent interactions [25]. The
69 oxygenous functional groups of GO make it a desirable basic candidate for the capture of acidic
70 CO_2, however, it needs some modifications to achieve satisfying CO_2 adsorption capacity. The
71 encouraging merit of GO is its high content of oxygen-bearing groups which can be easily
72 functionalized with nitrogenous compounds such as amine via nucleophilic substitution reactions
73 [26,27]. Amine-modified GO has higher CO_2 uptake potential than pure GO by virtue of the
74 high affinity of amino groups to CO_2 [28,29]. GO can be functionalized via whether
75 impregnation technique or grafting method. However, the impregnation method is the more easy
76 technique that improves the adsorption capability of the adsorbent than the grafting method [30].
77 Multitudinous researches have been conducted on the adsorption performance of GO. But, the
78 studies on amine-functionalized GO have been less carried out which necessitates further
79 investigations. It is expected that chemical rectification of GO with amine-containing agents
80 boosts the adsorption capacity of GO as CO_2 particles are bound to the pores via physical
81 interactions and to functional groups of the modified GO via chemical bonds[28].
82 In the present study, porous GO was impregnated with three types of amine functionalities
83 namely 3-aminopropyl-triethoxysilane (APTS), Piperazine (PIP), and ethanolamine (EA) to
84 investigate and compare their effectiveness in adsorption of CO_2. The possible mechanisms of
85 interaction of GO and various functionalities are described in Scheme 1. The fabricated

adsorbents were characterized for their surface functional groups, thermal stability, textural properties, and surface morphology. Furthermore, the thermodynamic and isothermal studies were also carried out for the large-scale application of the prepared adsorbents.

A

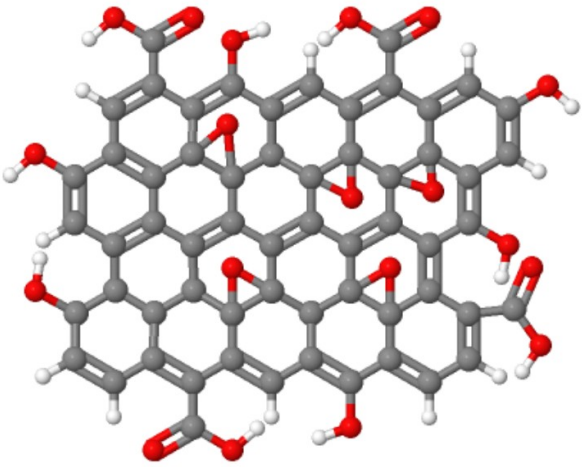

B

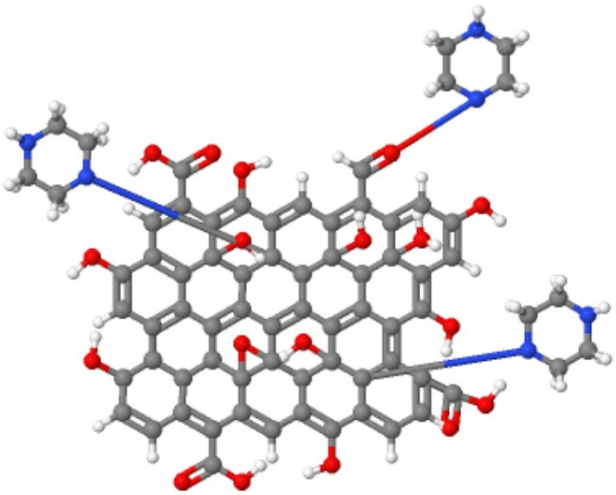

C

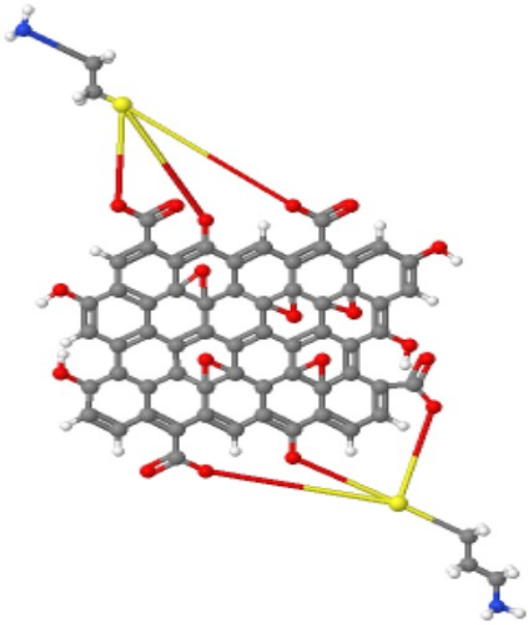

D

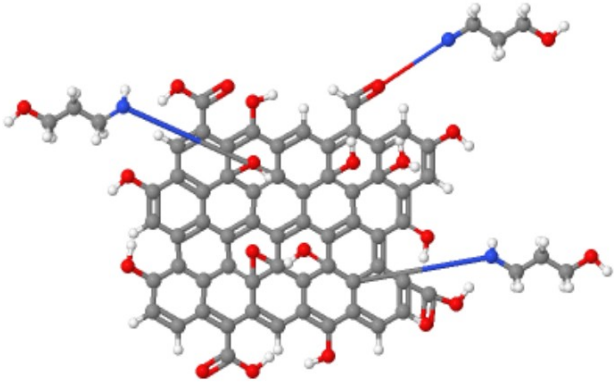

Scheme 1. The proposed reaction mechanism between GO (A) and amine-bearing agents: B) GO/PIP, C) GO/APTS, and D) GO/EA. (grey: carbon; white; hydrogen, red: oxygen, blue: nitrogen, yellow: sulfur)

2. MATERIALS AND METHODS

2.1. Materials

The graphite used in this research was obtained from Fluka and other chemicals including potassium permanganate, nitric acid (65%), sulfuric acid (98%), toluene (C_7H_8), 1,4 dioxane ($C_4H_8O_2$), and amine functionalities of EA ($C_9H_3C_{13}O$), APTS ($C_8H_{22}N_2O_3Si$), and PIP ($C_4H_{10}N_2$) were provided from Merck Co. Acetone (C_3H_6O) and ethanol (C_2H_6O) was purchased from Scharlau. Highly pure gases including carbon dioxide, helium, and nitrogen had been applied.

2.2. Synthesis of GO

The assembly of GO was carried out based on the famous procedure of Hummers [31] which can embed various oxygen-bearing functional groups at the edge and on the surface of the basal plane of graphene [20]. According to this method, nitric acid (HNO_3, 7.5 g) and graphite (7.5 g) was added to sulfuric acid (H_2SO_4, 360 ml) solution stirring at the rate of 500 rpm under the constant temperature of 0 ºC (the system was equipped with the ice-bath to set the reaction temperature at 0 ºC). After 1 h agitation, potassium permanganate ($KMnO_4$) was gently poured into the solution. The final solution was agitated for 3 h at 35 ºC. In the next step, H_2O_2 (3%) was gradually blended with the liquid composite during 30 min. The slurry was separated via filtration with a vacuum pump and the following centrifuging at 11000 rpm for 15 min. The remaining solid was refined by DI water and centrifuged until reaching a neutral sample, then, impurities were volatilized in the vacuum oven overnight at 60°C.

2.3. Synthesis of GO/APTS

20 ml APTS was decanted to the 80 ml toluene solution and the blend was stirred for 15 min at the rate of 500 rpm. Then, GO was added to the aqueous composite and was agitated at the constant rate of 500 rpm for 12 h under the stable temperature of 105 ºC. Then, the amine-functionalized GO was filtrated using a vacuum pump. In order to ensure the elimination of extra amine functionalities, the sample was rinsed with acetone several times. Finally, the prepared solid sample of GO/APTS was desiccated in an oven at the temperature of 80 ºC for 12 h.

2.4. Synthesis of GO/PIP

First, 3.73 g of PIP was dissolved in 1,4 dioxane (100 ml) and was stirred by a magnetic stirrer (500 rpm) at 15 ºC. GO was added to the obtained solution and was shaken under the temperature of 85 ºC for 21 h for well-mixing. The amine-functionalized GO has been filtered via a vacuum pump and washed with 1,4 dioxane, ethanol, and DI water to dissolve extra amines. The fabricated GO/PIP solid was left overnight in an oven at 80 ºC to be dewatered.

2.5. Synthesis of GO/EA

For the preparation of GO modified with EA, GO was poured into toluene (75 ml) and then ethanol solvent (1.5 mmol). The synthesized solution was agitated over a magnetic stirrer (500 rpm) for 18 h at the temperature of 80 ºC. Hereafter, the amine-doped sample was segregated by a vacuum pump and then rinsed with ethanol and DI water for the removal of unreacted amine groups. Finally, the synthesized GO/EA solid was desiccated via an oven at 80 ºC for 12 h.

2.6. The volumetric setup

A volumetric system was applied for the evaluation of adsorption experiments. The layout of the volumetric setup is represented in Figure 1. As it is obvious from the figure, the main part of the

system is composed of two stainless steel containers operating under elevated pressure which are known as pressure cell and adsorption cell. A water bath was used to provide the cells with a content temperature for adsorption of CO_2. In addition, the containers were provided with a temperature monitoring and pressure transformer for the record of temperature and pressure values during each test. Prior to the commencement of the experiments, solid samples became free of unwanted gases by keeping them under the temperature of 100 ºC for 12 h. Then, the prepared solid was sat in the adsorption unit and the apparatus was vacuumed by a vacuum pump device. For the estimation of the setup volume, helium gas was exploited as an inert gas. The test was begun by the entrance of CO_2 to the pressure cell until reaching an equilibrium condition.

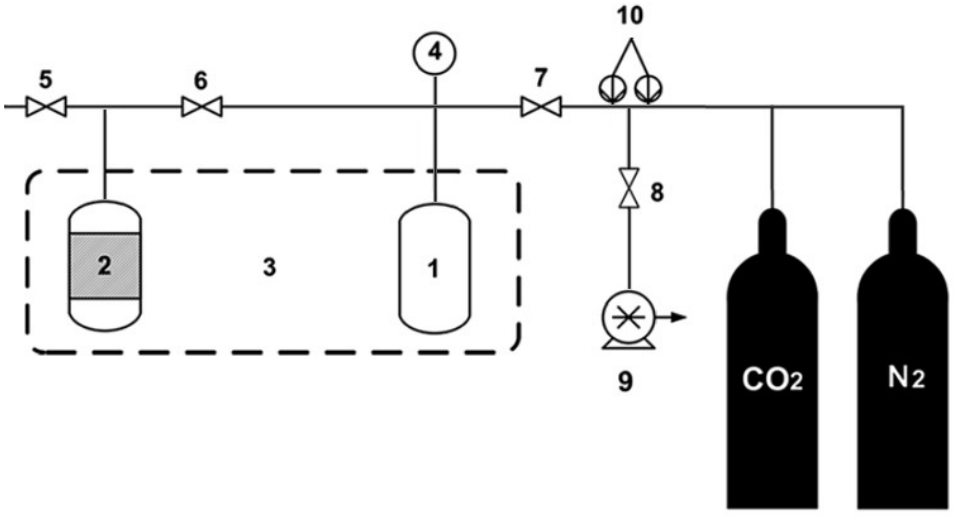

Figure 1. The experimental set-up:
(1) pressure cell; (2) adsorption cell; (3) water bath; (4) pressure gauge; (5-8) valves; (9) vacuum pump; (10) regulators.

2.7. Material Characterizing

The textural characteristics of the virgin and amine-modified GO series were estimated by N_2 adsorption-desorption isotherms at 77 K at the relative pressure (P/P0) range of 0.0001–0.99 using BELSORP mini II, Japan Inc instrument. The samples became devoid of any redundant substance under the temperature of 393 K for 15 h heretofore being exerted.

151 Further textural properties of the GO adsorbents including superficial area, mean pore diameter,
152 and pore volume were appraised by the Brunauer–Emmett–Teller (BET) method. Moreover, the
153 MP method was applied for the examination of micropore size distribution from the N_2
154 adsorption curve and the mesopore size distribution via the Barret–Joyner–Halenda (BJH)
155 technique.

156 The morphology of the GO, GO/PIP, GO/EA, and GO/APTS adsorbents were characterized by
157 high resolution scanning electron microscopy (SEM, VEGA IILMU, Tescan, Czech Republic)
158 analyzer at the voltage ranging from 1 to 30 kV. All solids were covered with a tenuous layer of
159 gold for premiere conductance.

160 For the goal of studying the superficial functional groups of the synthesized GO series and
161 proper modification of GO with amine-containing agents, the Fourier Transform Infrared
162 spectroscopy (Bruker Vertex-70 FTIR) was employed. In this regard, the solids were blended
163 with KBr and their patterns were tracked in the wavelength region of 400–4000 cm^{-1}.

164 The thermal resistance and dehydration quality of the adsorbents were measured by the
165 thermogravimetric analysis (TGA) (Mettler Toledo TGA-851, Switzerland) under the heat
166 treating of 10 °C/min in the temperature zone of 10-800 °C.

167 **2.8. Sips Isotherm Model**

168 Finding a proper isotherm model is a highly beneficial tool in estimation of the adsorption
169 equilibrium for commercial utilization of an adsorbent [32], expansion of its behavior under
170 different temperatures and even for different gases [33]. In order to address this point, the
171 experimental data were modeled on Sips isotherm. Sips or Langmuir–Freundlich isotherm is a
172 semi-empirical equation for predicting the equilibrium data of a real system [34]. Since the

common adsorbents used for the capture of gas have non-homogeneous surface and pore structures, semi-empirical isotherm patterns predict the data with better fitment to reality [35]. The equation of this model which is derived from the Langmuir and Freundlich isotherm models is provided below [13]:

$$q = q_m \frac{b\, p^{\frac{1}{n}}}{1 + b\, p^{\frac{1}{n}}} \qquad (1)$$

where q_m is the highest adsorbed CO_2 (mmol/g), b is the Langmuir constant, and n is the representative of the system heterogeneity. n=1 shows the Langmuir isotherm and values lower than 1 suggest the CO_2 chemisorption over a homogenous surface and values greater than 1 indicate the physisorption of CO_2 over a heterogeneous surface.

2.9. Adsorption Selectivity

The ideal adsorbed solution theory (IAST) predicts the selectivity of the composite gases system based on the isotherm of each element in a separate system [36]. Basically, IAST hypothesizes that the temperature of the system for the capture of an ideal gas mixture over the adsorbent is the same as the temperature of the single-component adsorption systems. This theoretical approach is considerably helpful since it eliminates the laboratory tests need for the evaluation and isothermal study of multiplex-gas systems [37]. The main assumptions of this theory are as follows: all gas components have identical interaction in the gas phase and have even access to the homogeneous adsorbent surface [38]. According to IAST, spreading pressures for pure and mixed gas are equivalent at equilibria [39]. In the current study, the selectivity of the adsorbent series toward CO_2 coexisting with N_2 was calculated. The spreading pressure in this system can be obtained according to equation (2), and Raoult's law for each component is described in

equations (3) and (4), and finally, the total amount of gas uptake is defined based on the equation (5).

$$\int_0^{P^0_{CO_2}} \frac{q_{CO_2}}{P} dP = \int_0^{P^0_{CO_2}} \frac{q_{N_2}}{P} dP = \frac{\pi A}{RT} \quad (2)$$

$$P\, y_{CO_2} = P^0_{CO_2} x_{CO_2} \quad (3)$$

$$y_{N_2} = P^0_{N_2} x_{N_2} \quad (4)$$

$$\frac{1}{q_t} = \frac{x_{CO_2}}{q_{CO_2}\left(P^0_{CO_2}\right)} + \frac{x_{N_2}}{q_{N_2}\left(P^0_{N_2}\right)} \quad (5)$$

In the above equations, q_t is the total adsorption capacity, and q_{CO2} and q_{N2} are the adsorption potential of the adsorbent for the capture of CO_2 and N_2, respectively. P^*_{CO2} and P^*_{N2} are the hypothetical pressure of CO_2 and N_2, respectively. x_i and y_i are representative of the molar proportion of gas components and A is the surficial area of the sorbent.

The adsorbent selectivity toward CO_2 is calculated via the below formula:

$$S_{CO_2/N_2} = \frac{x_{CO2}}{x_{N2}} \times \frac{y_{N2}}{y_{CO2}} \quad (6)$$

2.10. The Isosteric Heat of Adsorption

The adsorption equilibrium and the isosteric heat of adsorption (ΔH_{st}) are considered as the fundamental theoretical variables for the design and optimization of adsorptive removal of gases [40]. The adsorption of gases over porous adsorbents can lead to different ΔH_{st} as the surface coverage (or pressure) changes. First, a constant value of ΔH_{st} with an increment of surface coverage suggests homogeneous adsorption. Second, the reduction of ΔH_{st} with the development of surface loading alludes to the heterogeneity of adsorption. Third, the enhancement of ΔH_{st}

with the growth of adsorbent uptake suggests the strong lateral interactions between the gas molecules [41]. Moreover, it has been approximated by multitudinous researches that ΔH_{st} is independent of temperature in the systems employing porous adsorbent or having heterogeneous surface [42]. Various equations have been developed for the theoretic calculation of ΔH_{st}, among which, the Clausius-Clapeyron equation is the common and straight equation assuming the adsorption of ideal gases which is reliable under the low-pressure ranges [43]. The equation is:

$$\Delta H_{st} = R\left[\frac{d\ln p}{d\left(\frac{1}{T}\right)}\right]_q \qquad (7)$$

where ΔH_{st} (KJ/mol) is the isosteric heat of adsorption, T (K) is the temperature, P (bar) is pressure, and R is the ideal gas constant (J/mol K).

3. RESULTS AND DISCUSSIONS

3.1. Characterization of Adsorbents

The FTIR spectrum was carried out to study the functional groups of GO precursor and amine-impregnated GO series (see Figure 1).

Figure 1 confirms the proper synthesis of GO due to the presence of GO characteristics peaks at 3440, 1738, and 1020 cm^{-1} contributed to the O—H vibrancy in hydroxyl groups, —C=O vibrancy in carboxyl groups, and C—O—C stretching in epoxy groups, separately. The peak observed in 1649 cm^{-1} was dedicated to the vibrations of unoxidized sp_2-hybridized carbons of the graphite framework. The bands at 2923 and 2852 cm^{-1} were characteristics of the unsymmetrical and symmetrical vibrancy of CH_2 [20]. These bands were present in the spectra of all the modified samples with some changes in their intensity (mainly weakened) suggesting the incorporation and interaction of these oxygen functionalities with amine groups. The spread peak

238 around 3440 cm^{-1} for amine-doped adsorbents was pertained to the O—H stretching and N—H
239 stretching vibrancies which were overlapped. The bands at around 1095 and 790 cm^{-1} were
240 observed for GO/APTS sample which are representatives of vibrant Si—O—Si and Si—C
241 bonds, respectively [44]. The peaks at 1470 and 1650 cm^{-1} showed the vibration of C—N group
242 [45].

243 GO mainly contains hydroxyl and epoxy groups in its skeleton and carbonyl groups in the form
244 of carboxylic acid in the edges. The chemical interplay between amine groups and oxygenated
245 functional groups of GO occurs via i) covalent bonding between epoxy groups and amine
246 groups; ii) hydrogen bonding between hydroxyl groups and amines in the basal planes of GO
247 sheets [44] iii) amidation reactions between carboxyl and amine-bearing groups in edges of GO
248 sheets. Furthermore, hydroxyl and carboxylic acid functional groups of GO may interact via
249 hydrogen bonds and electrostatic interactions [46]. According to the mentioned explanations
250 along with the spectra pattern of GO samples, well impregnation of amine-containing chemicals
251 on the GO surface was verified.

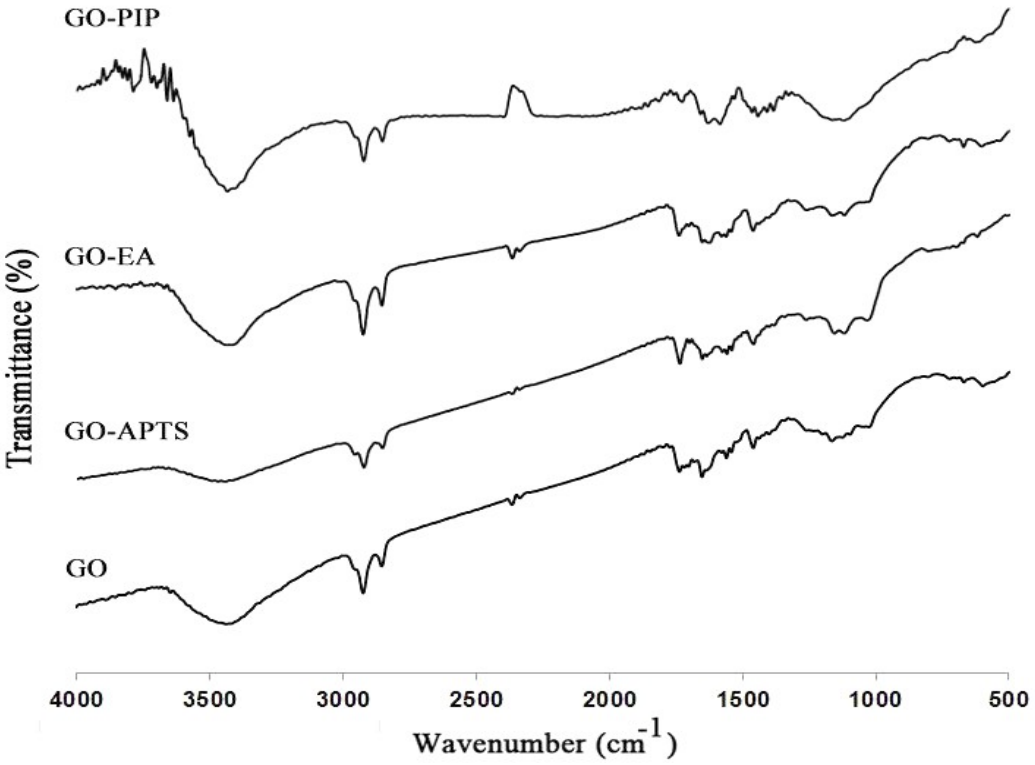

252

253 **Figure 1.** FTIR spectra of the unmodified and modified GO adsorbents

254 A favorable adsorbent for CO_2 capture should possess desirable stability. Indeed, the thermal
255 stability of adsorbents enriched with amine-oriented agents is highly important, in particular, in
256 the desorption stage which is usually conducted under higher temperatures [18,47].

257 Figure 2 summarizes TGA thermograms of pristine and amine-functionalized GO series. The
258 three-stage decomposition pattern is observable for all adsorbents. The initial decomposition
259 stage emerged below 100 ºC for all adsorbents which was ascribed to the evaporation of
260 physisorbed moisture and other fugacious elements [48]. The further decomposition stages of
261 GO occurred at temperatures of about 205 ºC and 310 ºC with mass loss of about 13% and 11%,
262 respectively. The second decomposition region was related to the rupture of unstable oxygenated
263 functional groups namely OH, CO, and COO^- groups [49]. The third decomposition region can
264 be assigned to the dissociation of resistant oxygenated functional groups namely acidic

carboxylic and lactones. The mass loss in the second phase, in the temperature range of 170 ºC to 600 ºC, was 30.53 % for GO/ATPS, 9 % for GO/EA, and 17.35 % for GO/PIP. In this stage, deoxygenation and dissociation of physically adsorbed amines agents happened since EA, PIP, and APTS were not quite involved in the grafting reaction and some unreacted agents remained on surfaces [50]. The weight reduction in the third region at temperatures of 600 ºC, 240 ºC, and 430 ºC was around 3.17 %, 17.46 %, and 8.99 % for GO/ATPS, GO/EA, and GO/PIP, respectively, suggesting the pyrolysis of physisorbed amine groups. The TGA results unfolded that the thermostability of adsorbents improved after modification with the amine-containing agents [51].

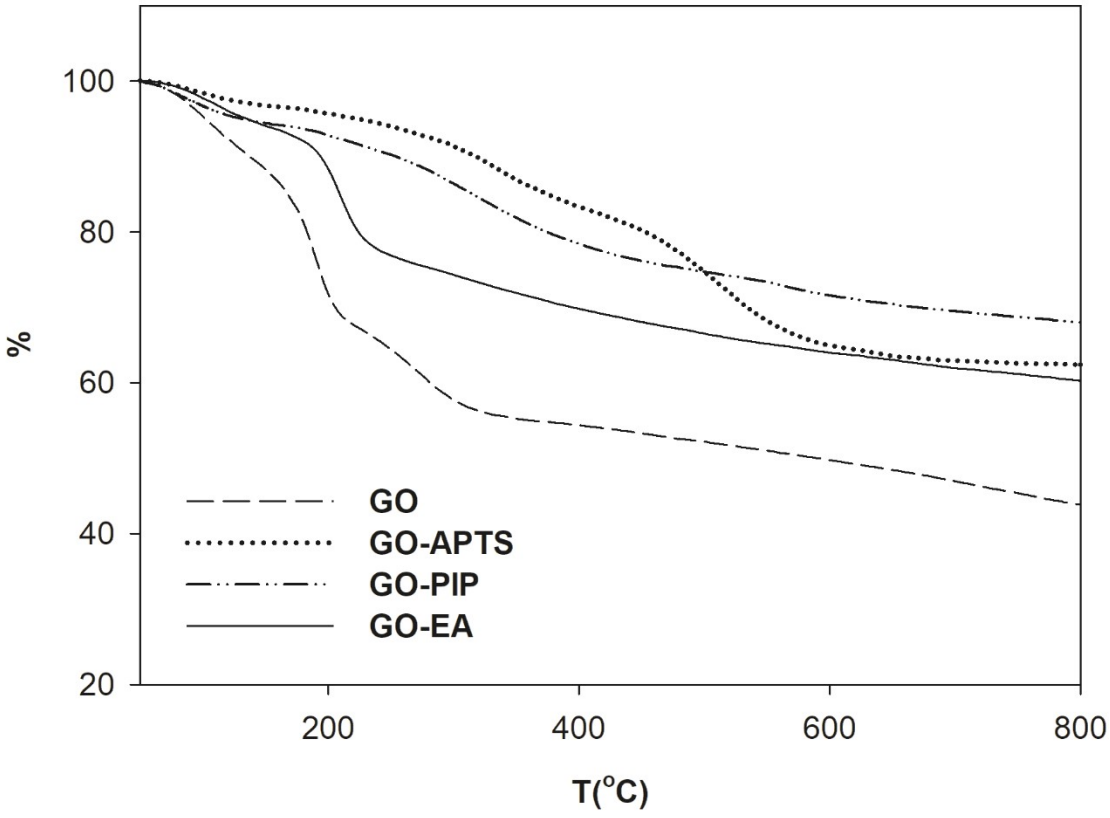

Figure 2. TGA analysis of the unmodified and modified GO adsorbents

276 The high-resolution surface morphology of the synthesized GO samples is presented in Figure 3.
277 The unmodified GO adsorbent had a flacked structure with flocculent and wrinkled morphology
278 which is the typical morphology of GO. This morphology is stemmed from the oxidation of
279 graphite clusters in which the irregularity of the stacks of the graphite clusters leads to a
280 disrupted structure [52]. The modified GO sorbents showed morphologies with less stack and
281 more wrinkles than pristine GO. These records convey that amine functionalities extended the
282 interlayers of GO which were linked via peroxide-like linkages [26,53]. Furthermore, the results
283 indicated the successful chemical modification of the GO surface.

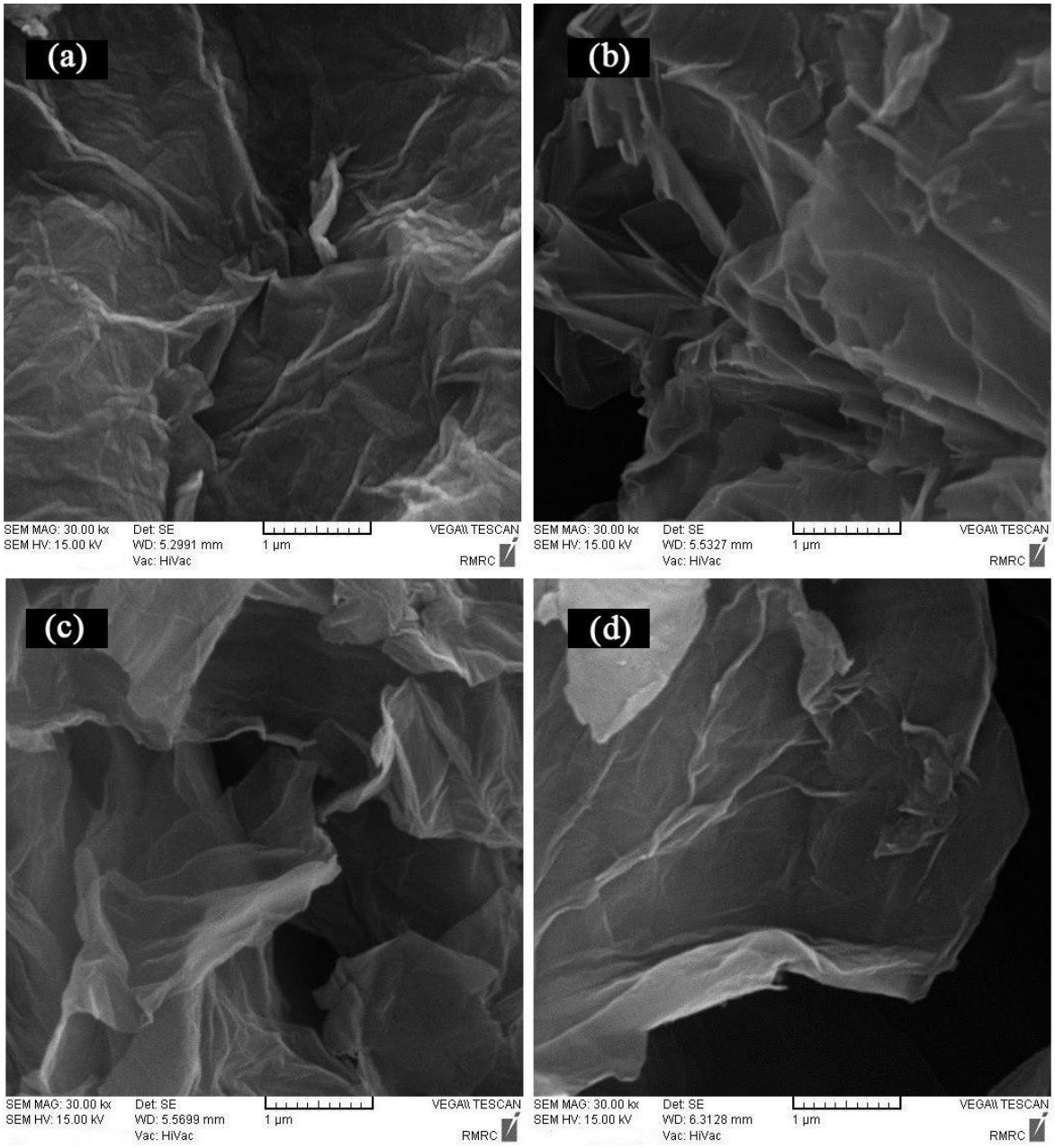

Figure 3. SEM images of a) GO, b) GO-APTS, c) GO-PIP, and d) GO-EA

The functionalization of adsorbents gives new physical characteristics to them which affects the capability of adsorbents for adsorption of CO_2. The physical characteristics of the assembled adsorbents comprising the surficial area and pore volume were quantified using N_2 adsorption-desorption isotherm. Figure 4 confirms the dominance of the mesoporosity of the adsorbents as

290 they exhibit an IV-type isotherm with a hysteresis loop. The N_2 adsorption-desorption curve of
291 GO shifted to the lower values after grafting with amine-oriented agents. The main reason was
292 the pore filling via modification by aminated agents, giving rise to the reduction of free pores
293 available for N_2 molecules. The diminution of pore volume and surface area asserted the
294 successful insertion of amine to the GO matrix [54]. Based on the BET results (Table 1), the pore
295 diameter of all adsorbents was between 2 and 50 nm, confirming the mesoporous structure of the
296 synthesized GO series. The results of BJH and MP methods presented in Figure 5 imply the
297 mesopore and micropore size distribution in samples. Figure 5A indicates the mesopore size
298 distribution of samples was between 2 and 5 nm. According to Figure 5 B, micropores are
299 distributed more abundantly around 0.7~1.2 nm for GO and GO/APTS samples and around
300 1.6~2 nm for GO/PIP and GO/EA samples.

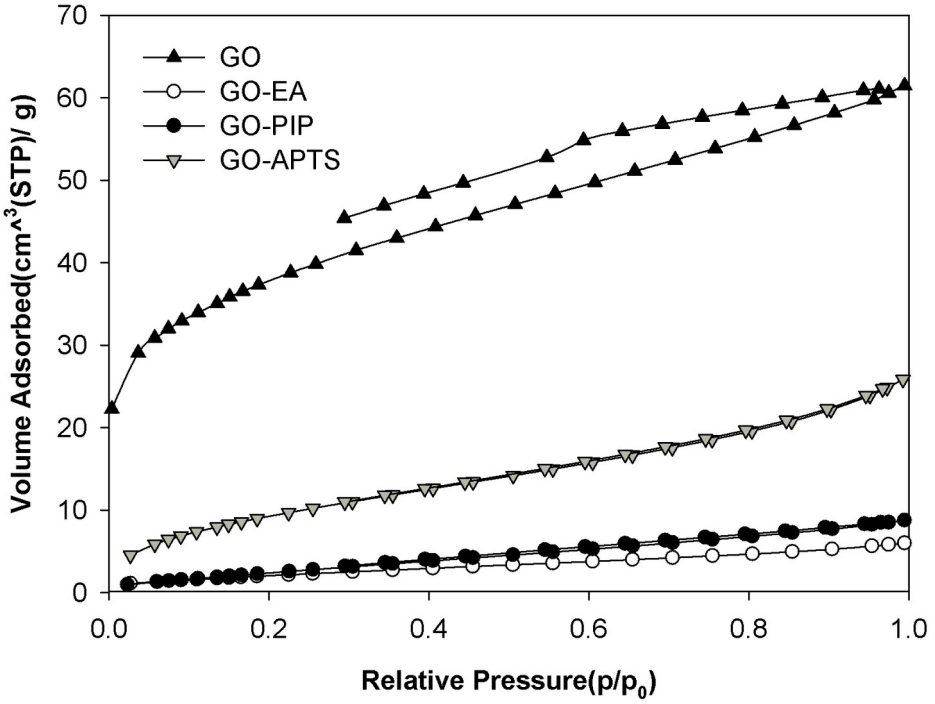

301

302 **Figure 4.** N_2 adsorption/desorption of the unmodified and modified GO adsorbents

Table 1. The surface characteristics of the unmodified and modified GO adsorbents

Sample	S_{BET} (m^2/g)	V_{mic} (cm^3/g)	V_{mes} (cm^3/g)	V_{total} (cm^3/g)	V_{mic} (%)	D_p (nm)
GO	134.51	0.082	0.012	0.094	0.302	2.81
GO-APTES	36.44	0.026	0.013	0.039	0.662	4.36
GO-PIP	10.39	0.009	0.003	0.013	0.706	5.18
GO-EA	7.91	0.006	0.002	0.009	0.690	4.65

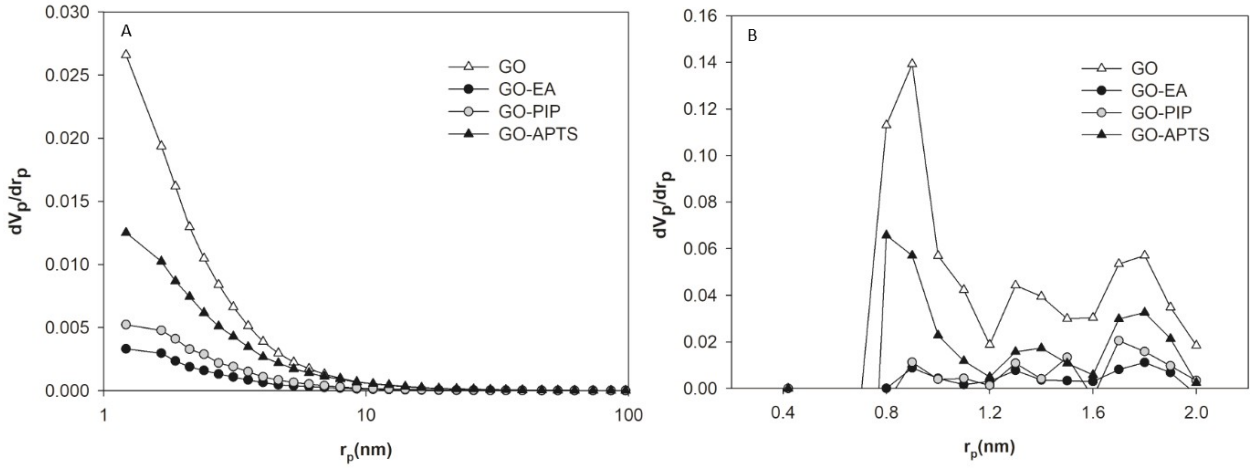

Figure 5. The pore size distribution by A) BJH and B) MP methods

3.2. Adsorption experiments

The CO_2 adsorption uptake of GO, GO/APTS, GO/PIP, and GO/EA was measured at 298, 308, and 318 K under the pressure range of 0-14 bar (Figure 5). It can be perceived that the CO_2 capture capacity of all GO sets was detracted as the temperature heightened from 298 to 318 K. Because the adsorption of CO_2 was exothermal, thus, higher temperature hindered the adsorption of CO_2 [55]. Moreover, with the rise of pressure, the CO_2 adsorption quantity increased for all prepared samples. The adsorption capacity of adsorbents increased sharply at low pressures and

313 grew slightly at higher pressures. Under the high-pressure zone, pores of adsorbents were
314 engaged in CO_2 molecules which resulted in the decrement of the rate of adsorption.

315 It is also evident from Figure 6 that amine-doped GO samples presented higher CO_2 adsorption
316 capacity compared to the virgin GO. According to papers, a high volume of micropore is
317 concerned with high CO_2 adsorption capacity [56]. In this regard, it was expected that GO had
318 the highest CO_2 uptake capacity due to its better physical properties. However, the physical
319 properties of the samples (Table 1) contradicted this point. The reason for this behavior is the
320 amelioration of functionalities of the amine-anchored adsorbents that compensates for the
321 physical properties. The basicity of GO improved via deposition of basic amine groups giving it
322 a higher affinity toward acidic CO_2. This interaction is called Lewis acid-base interaction, in
323 which, amine groups are recognized as Lewis base for their pair electrons and CO_2 is classified
324 as a Lewis acid due to the absence of paired electron [55].

325 Among the modified samples, GO/APTS showed better CO_2 adsorption potential than GO/PIP
326 and GO/EA, which may be attributed to its both better surface characteristics and basicity.
327 GO/APTS had the highest surface area and micropore volume in comparison with the GO/PIP
328 and GO/EA samples. In addition, it was assumed that the existence of electron-donating oxygen
329 atoms and primary amine groups of APTS donated GO/APTS a strong basic character among the
330 other amine-modified adsorbents [6,51]. PIP contains two secondary amines in its structure,
331 which provides it with higher number of active sites compared to EA, having a primary amine in
332 its chain.

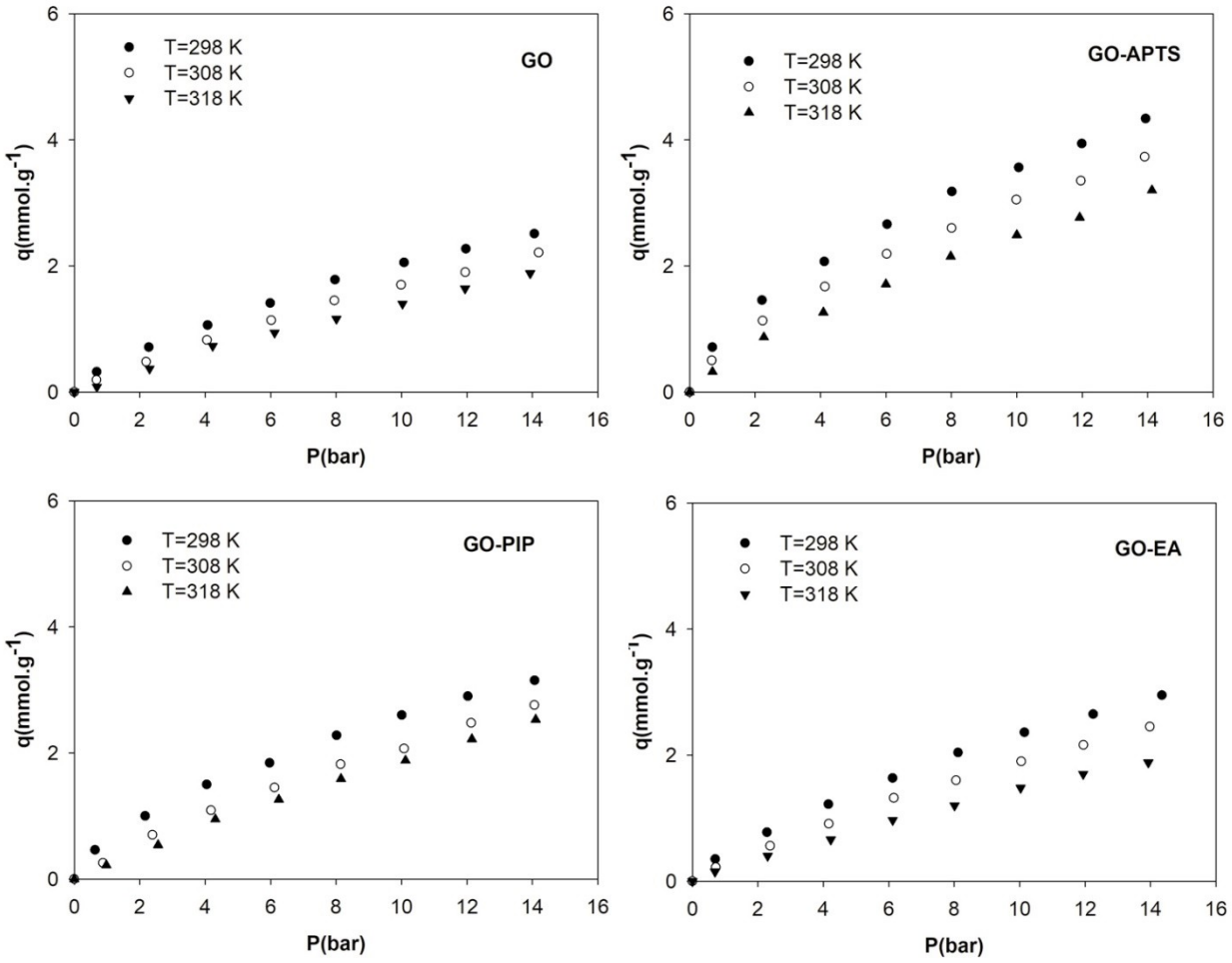

Figure 6. The CO_2 adsorption capacity of prepared adsorbents at different temperatures and pressures

3.3. Isotherm study

The Sips isotherm was fitted to predict experimental data of CO_2 and N_2 adsorption over the as-prepared GO series (see Figure 7). The constants and variables of the Sips model are tabulated in Table 2 which indicates that the Sips model correlated the experimental data of CO_2 capture with great coefficients of 0.999. The Sips model predicted the adsorption of N_2 over N-doped adsorbents precisely (correlation coefficient=1). The values of n which are higher than the unit indicated the physisorption of gas molecules over the heterogeneous adsorbents.

343 It was also implied from the table that GO/APTS and unmodified GO adsorbents had the best
344 adsorption capacity for the capture of CO_2 and N_2, respectively. The highest affinity of
345 GO/APTS for CO_2 capture might be attributed to its better physical and chemical properties. In
346 the case of chemical characteristics, the improvement of the basicity of GO gave rise to the
347 higher CO_2 adsorption. To be more specific, the electron donor amine-anchored GO adsorbents
348 revealed the higher CO_2 adsorption potential, among which, APTS manifested the best
349 performance by reason of the presence of primary amine groups along with the electron donor
350 methyl groups in its structure. The lowest CO_2 adsorption capacity of GO/PIP can be associated
351 with the amine aromatic ring which has the least basicity properties giving rise to the less
352 improved adsorption capacity [55]. Moreover, it can be perceived that the quantity of captured
353 CO_2 increased aligned with the enhancement of the molecular weight of amine-entailed
354 chemicals [57]. In addition, the highest BET exterior area of GO/APTS among the other amine-
355 modified samples made GO/APTS the most favorable adsorbent. As was mentioned, GO showed
356 the highest N_2 adsorption uptake among the as-prepared samples implying the unreactive nature
357 of N_2 toward amine-modified adsorbents.

358 Table 3 indicates the reports of some recent studies in regard to the CO_2 adsorption potential of
359 various amine-doped graphene adsorbents. The results vividly demonstrate the remarkable
360 adsorption potential of the as-prepared samples in this study, with the superior adsorption
361 capability related to the GO-APTS at the environmental condition. From an industrial
362 perspective, an adsorbent working under the ambiance conditions is valuable since it is difficult,
363 energy-intensive, and costly to employ adsorbent operating at severe conditions (high
364 temperature and pressure) for large-scale applications. Therefore, the results of the present

research show the well-application of our modified GO adsorbents in comparison with other amine-functionalized GO prepared via different methods.

Table 2. The parameters of the Sips isotherm model

Gas type	Adsorbent	q_m(mmol/g)	b	n	R^2	q_{exp} (mmol/g) at 298K and 1bar
CO_2	GO	13.263	0.030	1.284	0.999	0.39
	GO-APTS	43.114	0.021	1.574	0.999	0.90
	GO-PIP	30.048	0.021	1.521	0.999	0.61
	GO-EA	16.260	0.027	1.253	0.999	0.45
N_2	GO	7.409	0.029	1.182	0.997	0.23
	GO-APTS	3.400	0.027	1.131	1.000	0.09
	GO-PIP	5.117	0.026	1.006	1.000	0.14
	GO-EA	5.166	0.031	1.023	1.000	0.16

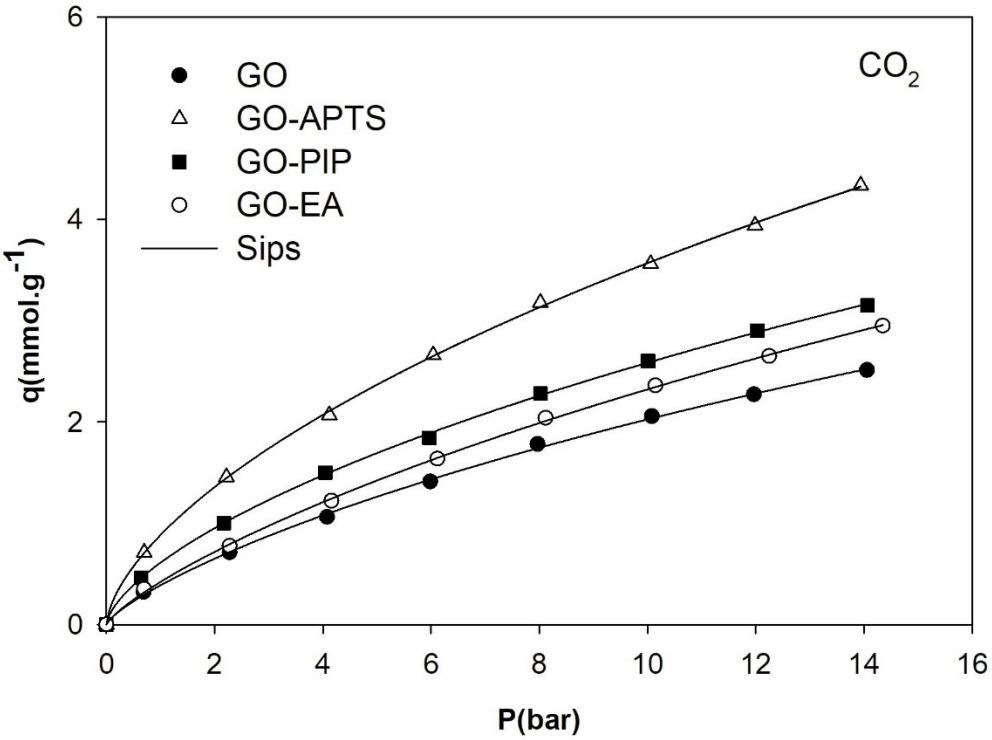

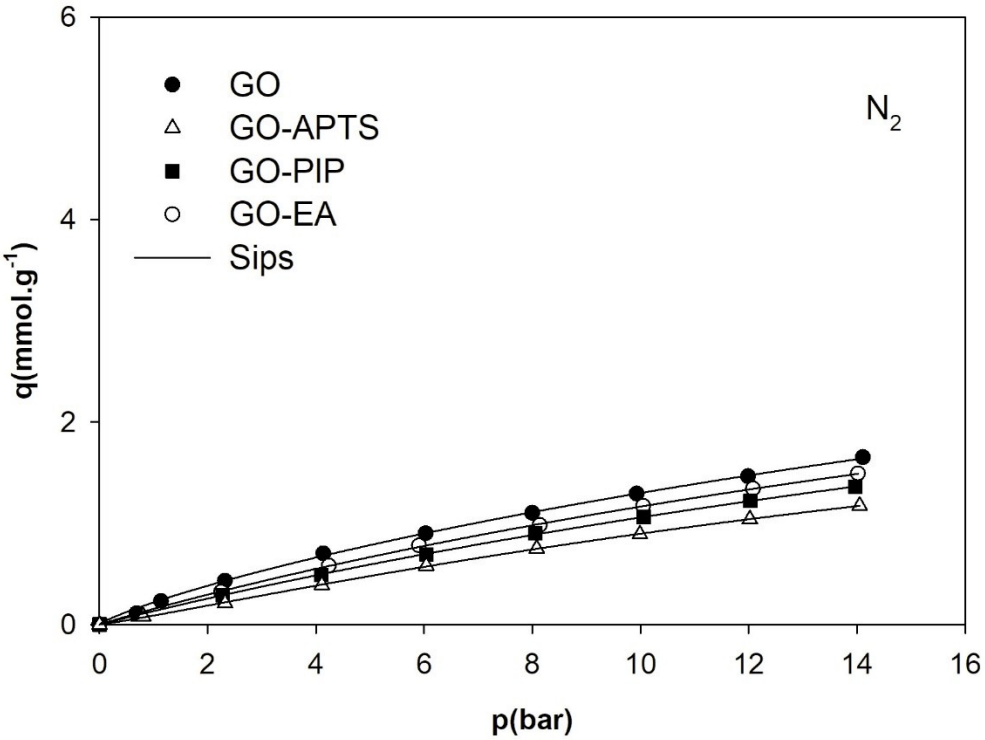

369

370 **Figure 7.** The Sips isotherm of adsorption of CO_2 and N_2 over the GO-based adsorbent

371 **Table 3. The CO_2 adsorption capacity of amine-functionalized adsorbents**

Adsorbent	CO_2 adsorption capacity (mmol/g)	Experimental conditions	Ref
GO-APTS	0.90	298 K, 1 bar	Present study
GO-PIP	0.61	298 K, 1 bar	
GO-EA	0.45	298 K, 1 bar	
PEI-GO	2.91	348 K	[8]
EDA-GO	1.18	298 K, 1 bar	[26]
PEI-GO	0.49	273 K, 1 bar	[58]
TEPA-GO	1.22	338 K, 1 bar	[59]
AMS-5% RGO	1.68	323 K	[60]
TEPA(3%)/GO	2.08	298 K, 30 bar	[61]
TEPA(5%)/GO	1.95	298 K, 30 bar	
TEPA(10%)/GO	1.20	298 K, 30 bar	
TEPA(50%)/GO	0.98	298 K, 30 bar	
PEI(60%)-GO	0.74	298 K, 1 bar	[62]
APTS-Gr	1.16	303 K, 1 bar	[63]
Semi-coke/GO/DEA	7.11	298 K, 30 bar	[64]
APTES-GO	1.50	303 K, 1 bar	[7]
PTES-GO	1.79	303 K, 15 bar	[65]

372

373 **3.4. The isosteric heat of adsorption**

Figure 8 presents the isosteric heat of adsorption of CO_2 over synthesized GO series as a function of superficial coating. Decreasing patterns with different slopes were obtained for all prepared samples representing the exothermal reaction of CO_2 with active sites of the solid adsorbents. The figure also signifies that the isosteric heat of CO_2 adsorption relied on the surface occupation. This trend shows the heterogeneous adsorption reaction, in which, interactions between CO_2 and active sites proceeded unevenly [66]. In addition to the mentioned points, the isosteric heat of adsorption is also a key parameter to help in order to figure out the mechanism of adsorption. The physical adsorption, which is regarded as weak interactions between adsorbate and adsorbent, have the heat in between 25-50 kJ/mol, while, the chemical adsorption, which is known as strong adsorption, possesses the heat of adsorption in between 60–90 kJ/mol [67]. Accordingly, the adsorption of CO_2 over virgin and aminated GO was categorized as physisorption.

It is also obvious from Figure 8 that the isosteric heat of adsorption decreased quickly at low surface coating and reduced slightly at high surface occupation. This behavior suggested the dominance of adsorbent-adsorbate reactions at a low loading of CO_2. With the expansion of CO_2 loading, the active sites of adsorbents were occupied and adsorbate-adsorbate interactions became the main interactions [68].

Among the synthesized adsorbents, GO/APTS revealed the highest heat of adsorption under any ranges of surface coverage. The availability of more active sites (primary amine groups) may be concerned with this observation as was reported by Watabe et al [69]. It is known that the high isosteric heat of adsorption intensifies the required energy consumption for the regeneration of adsorbent. Although the greater isosteric heat of adsorption is an unfavorable parameter in the

396 regeneration stage, it escalated the purity of adsorbed CO_2 owing to the enhancement of
397 adsorbent selectivity [70].

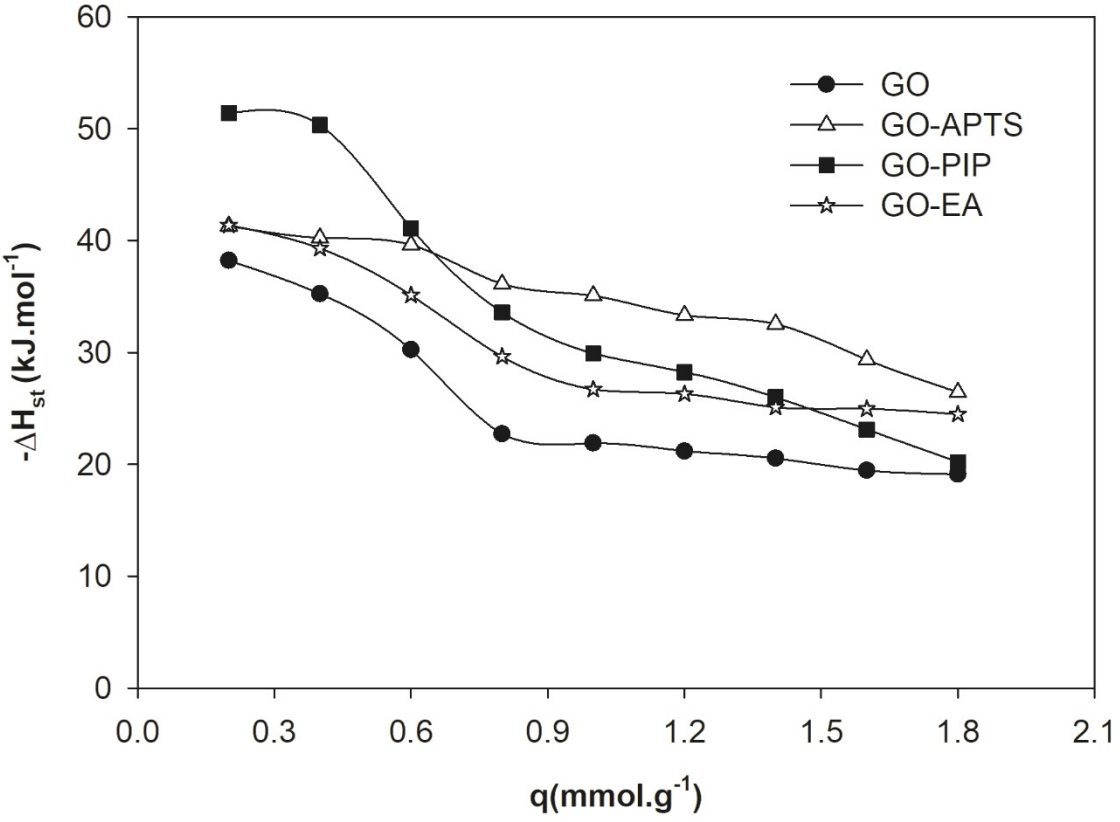

398

399 **Figure 8.** The isosteric heat of CO_2 adsorption versus surface loading

400 **3.5. Selectivity**

401 The selectivity of an adsorbent for the capture of CO_2 is a high-priority characteristic as this
402 momentous greenhouse gas exhausted from industrial flue exists in accompany with other gases.
403 Figure 9 depicts the selectivity of the unmodified and alkyl-modified GO adsorbents toward CO_2
404 in the presence of N_2 (N_2:85%) and Table 4 itemizes the selectivity of adsorbents for CO_2 at
405 ambiance conditions. As the figure illustrates, the selectivity of amine-treated adsorbents toward
406 CO_2 was significant under low-pressure regimes and reduced promptly with the increase of

pressure from 0.01 to 0.25 bar. The better selectivity of amine-decorated adsorbents is vivid from the outcomes, confirming the successful modification of GO. The highest selectivity of GO/APTS among the modified samples supports the improved characteristics of the adsorbent via the insertion of reactive primary amine groups to GO.

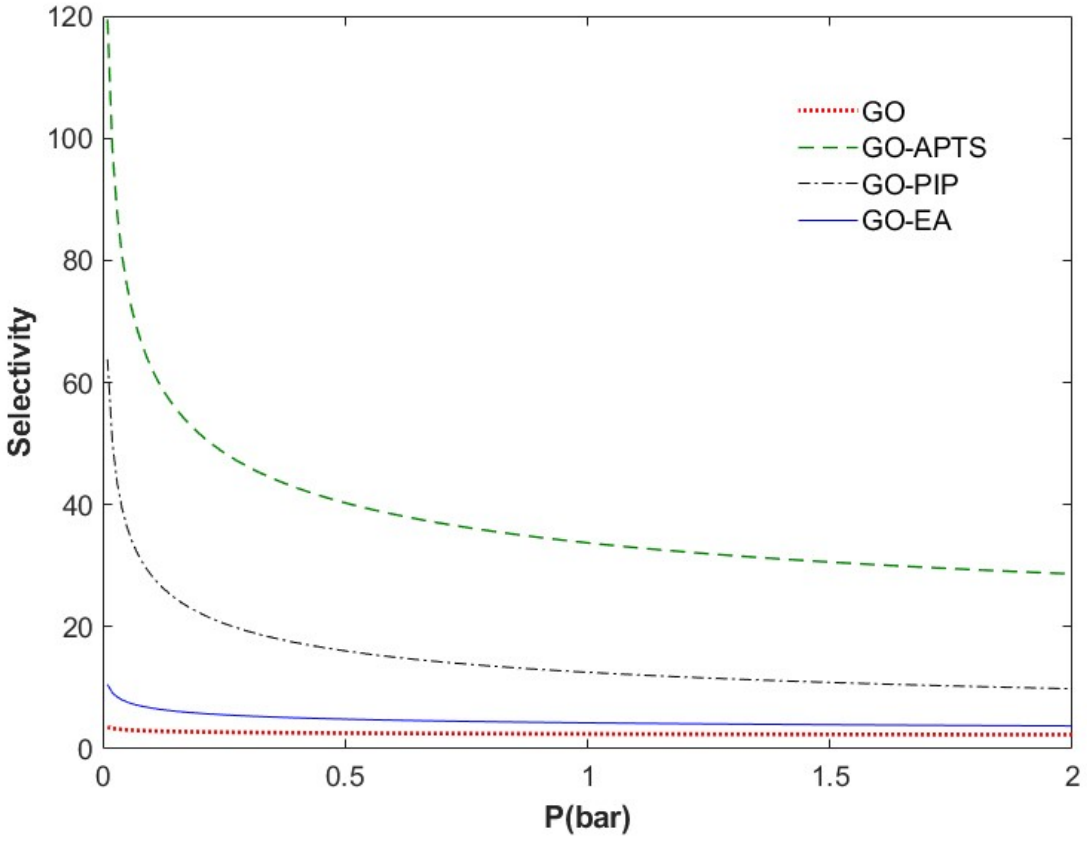

Figure 8. The selectivity of the unmodified and modified GO adsorbents for CO_2 over N_2

Table 4. The CO_2 selectivity of the adsorbents at CO_2: N_2 =0.15:0.85, 298 K, 1 bar

Adsorbent	Selectivity (%)
GO	2.44
GO/APTS	33.73
GO/PIP	12.54
GO/EA	4.26

4. CONCLUSION

Functionalization of GO precursor with three amine functionalities (APTS, PIP, EA) were carried out in order to capture CO_2. The experimental tests were considered under different temperatures (298, 308, and 318 K) and pressures (0-14 bar) in a dynamic adsorption setup. The proper functionalization was validated by analyzing tools of FTIR, TGA, SEM, BET, BJH, and MP. Indeed, the as-fabricated aminated samples had a mesoporous structure with remarkable thermal resistance and a lower specific surficial area than pristine GO. The best performance was dedicated to GO/APTS adsorbent with the maximum CO_2 adsorption capacity of 43.114 mmol/g obtained by the Sips isotherm model and the IAST selectivity of 33.73 % toward CO_2 (CO_2:N_2:0.15:0.85). This great performance was due to: 1) its great physicochemical qualities i.e. highest surface area (36.44 m^2/g) and molecular weight, 2) the existence of electron-donor primary amine and methyl groups in APTS result in intense affinity toward the acidic CO_2. The adsorption of CO_2 was classified as physical adsorption since the isosteric heat of adsorption for all adsorbents was lower than 50 KJ/mol. The result of this study confirmed the importance of the proper choice of a modifying agent which can drastically alter the performance of the adsorbent.

5. REFERENCE

[1] F. Gao, J. Bin Zhang, C.P. Li, T.R. Huo, X.H. Wei, Supramolecular binding of amines with functional magnesium tetraphenylporphyrin for CO2 capture, Chinese Chem. Lett.

24 (2013) 249–252. doi:10.1016/j.cclet.2013.01.043.

[2] K. Kole, S. Das, A. Samanta, S. Jana, Parametric Study and Detailed Kinetic Understanding of CO 2 Adsorption over High-Surface-Area Flowery Silica Nanomaterials , Ind. Eng. Chem. Res. (2020). doi:10.1021/acs.iecr.0c04531.

[3] C.-H. Yu, C.-H. Huang, C.-S. Tan, A review of CO2 capture by absorption and adsorption, Aerosol Air Qual. Res. 12 (2012) 745–769.

[4] L. Yang, C. Shi, L. Li, Y. Li, High-throughput model-building and screening of zeolitic imidazolate frameworks for CO2 capture from flue gas, Chinese Chem. Lett. 31 (2020) 227–230. doi:10.1016/j.cclet.2019.04.025.

[5] M.G. Yıldız, T. Davran-Candan, M.E. Günay, R. Yıldırım, CO2 capture over amine-functionalized MCM-41 and SBA-15: Exploratory analysis and decision tree classification of past data, J. CO2 Util. 31 (2019) 27–42.

[6] W. Zhang, E. Gao, Y. Li, M.T. Bernards, Y. He, Y. Shi, CO2 capture with polyamine-based protic ionic liquid functionalized mesoporous silica, J. CO2 Util. 34 (2019) 606–615.

[7] J. Pokhrel, N. Bhoria, S. Anastasiou, T. Tsoufis, D. Gournis, G. Romanos, G.N. Karanikolos, CO2 adsorption behavior of amine-functionalized ZIF-8, graphene oxide, and ZIF-8/graphene oxide composites under dry and wet conditions, Microporous Mesoporous Mater. 267 (2018) 53–67.

[8] Y. He, Y. Xia, J. Zhao, Y. Song, L. Yi, L. Zhao, One-step fabrication of PEI-modified GO particles for CO 2 capture, Appl. Phys. A. 125 (2019) 160.

[9] Y. Chen, G. Lin, S. Chen, Preparation of a Solid Amine Microspherical Adsorbent with High CO2Adsorption Capacity, Langmuir. 36 (2020) 7715–7723. doi:10.1021/acs.langmuir.9b03694.

[10] W. Zhang, H. Liu, C. Sun, T.C. Drage, C.E. Snape, Performance of polyethyleneimine–silica adsorbent for post-combustion CO2 capture in a bubbling fluidized bed, Chem. Eng. J. 251 (2014) 293–303.

[11] Z. Liu, Y. Teng, K. Zhang, H. Chen, Y. Yang, CO2 adsorption performance of different amine-based siliceous MCM-41 materials, J. Energy Chem. 24 (2015) 322–330.

[12] I. Sreedhar, R. Aniruddha, S. Malik, Carbon capture using amine modified porous carbons derived from starch (Starbons®), SN Appl. Sci. 1 (2019) 463.

[13] S. Khalili, B. Khoshandam, M. Jahanshahi, Synthesis of activated carbon/polyaniline nanocomposites for enhanced CO 2 adsorption, RSC Adv. 6 (2016) 35692–35704.

[14] F.-Q. Liu, W. Li, J. Zhao, W.-H. Li, D.-M. Chen, L.-S. Sun, L. Wang, R.-X. Li, Covalent grafting of polyethyleneimine on hydroxylated three-dimensional graphene for superior CO 2 capture, J. Mater. Chem. A. 3 (2015) 12252–12258.

[15] M. Oschatz, M. Antonietti, A search for selectivity to enable CO 2 capture with porous adsorbents, Energy Environ. Sci. 11 (2018) 57–70.

[16] D.K. Yoo, T.-U. Yoon, Y.-S. Bae, S.H. Jhung, Metal-organic framework MIL-101 loaded with polymethacrylamide with or without further reduction: Effective and selective CO2 adsorption with amino or amide functionality, Chem. Eng. J. 380 (2020) 122496.

[17] J. Han, L. Zhang, B. Zhao, L. Qin, Y. Wang, F. Xing, The N-doped activated carbon

477 derived from sugarcane bagasse for CO2 adsorption, Ind. Crops Prod. 128 (2019) 290–
478 297.

479 [18] H. Zhao, X. Luo, H. Zhang, N. Sun, W. Wei, Y. Sun, Carbon−based adsorbents for post−
480 combustion capture: a review, Greenh. Gases Sci. Technol. 8 (2018) 11–36.

481 [19] V. Irani, A. Tavasoli, M. Vahidi, Preparation of amine functionalized reduced graphene
482 oxide/methyl diethanolamine nanofluid and its application for improving the CO2 and
483 H2S absorption, J. Colloid Interface Sci. 527 (2018) 57–67.

484 [20] S.-M. Hong, S.H. Kim, K.B. Lee, Adsorption of carbon dioxide on 3-aminopropyl-
485 triethoxysilane modified graphite oxide, Energy & Fuels. 27 (2013) 3358–3363.

486 [21] S.N. Kudahi, A.R. Noorpoor, N.M. Mahmoodi, Determination and analysis of CO2
487 capture kinetics and mechanisms on the novel graphene-based adsorbents, J. CO2 Util. 21
488 (2017) 17–29.

489 [22] J. Hu, G. Kong, Y. Zhu, C. Che, Ultrafast room-temperature reduction of graphene oxide
490 by sodium borohydride, sodium molybdate and hydrochloric acid, Chinese Chem. Lett.
491 (2020). doi:10.1016/j.cclet.2020.03.045.

492 [23] U. Rana, S. Malik, Graphene oxide/polyaniline nanostructures: transformation of 2D sheet
493 to 1D nanotube and in situ reduction, Chem. Commun. 48 (2012) 10862–10864.

494 [24] M. Khajouei, M. Najafi, S.A. Jafari, Development of ultrafiltration membrane via in-situ
495 grafting of nano-GO/PSF with anti-biofouling properties, Chem. Eng. Res. Des. 142
496 (2019) 34–43. doi:10.1016/j.cherd.2018.11.033.

497 [25] S. Gadipelli, Z.X. Guo, Graphene-based materials: Synthesis and gas sorption, storage and

498 separation, Prog. Mater. Sci. 69 (2015) 1–60.

499 [26] A. Pruna, A.C. Cárcel, A. Benedito, E. Giménez, Effect of synthesis conditions on CO2
500 capture of ethylenediamine-modified graphene aerogels, Appl. Surf. Sci. 487 (2019) 228–
501 235.

502 [27] M.A. Worsley, T.Y. Olson, J.R.I. Lee, T.M. Willey, M.H. Nielsen, S.K. Roberts, P.J.
503 Pauzauskie, J. Biener, J.H. Satcher Jr, T.F. Baumann, High surface area, sp2-cross-linked
504 three-dimensional graphene monoliths, J. Phys. Chem. Lett. 2 (2011) 921–925.

505 [28] S. Khalili, A.A. Ghoreyshi, M. Jahanshahi, K. Pirzadeh, Enhancement of carbon dioxide
506 capture by amine−functionalized multi−walled carbon nanotube, Clean–Soil, Air, Water.
507 41 (2013) 939–948.

508 [29] R. Aghehrochaboki, Y.A. Chaboki, S.A. Maleknia, V. Irani, Polyethyleneimine
509 functionalized graphene oxide/methyldiethanolamine nanofluid: Preparation,
510 characterization, and investigation of CO2 absorption, J. Environ. Chem. Eng. 7 (2019)
511 103285.

512 [30] M.B. Yue, L.B. Sun, Y. Cao, Z.J. Wang, Y. Wang, Q. Yu, J.H. Zhu, Promoting the CO2
513 adsorption in the amine-containing SBA-15 by hydroxyl group, Microporous Mesoporous
514 Mater. 114 (2008) 74–81.

515 [31] W.S. Hummers Jr, R.E. Offeman, Preparation of graphitic oxide, J. Am. Chem. Soc. 80
516 (1958) 1339.

517 [32] S. Khalili, B. Khoshandam, M. Jahanshahi, Synthesis of activated carbon / polyaniline
518 nanocomposites for enhanced CO 2 adsorption †, RSC Adv. 6 (2016) 35692–35704.

519 doi:10.1039/C6RA00884D.

520 [33] I.A.A.C. Esteves, M.S.S. Lopes, P.M.C. Nunes, J.P.B. Mota, Adsorption of natural gas
521 and biogas components on activated carbon, Sep. Purif. Technol. 62 (2008) 281–296.

522 [34] K.Y. Foo, B.H. Hameed, Insights into the modeling of adsorption isotherm systems,
523 Chem. Eng. J. 156 (2010) 2–10. doi:10.1016/J.CEJ.2009.09.013.

524 [35] S. Garcia, J.J. Pis, F. Rubiera, C. Pevida, Predicting mixed-gas adsorption equilibria on
525 activated carbon for precombustion CO2 capture, Langmuir. 29 (2013) 6042–6052.

526 [36] E. Sauer, J. Gross, Prediction of Adsorption Isotherms and Selectivities: Comparison
527 between Classical Density Functional Theory Based on the Perturbed-Chain Statistical
528 Associating Fluid Theory Equation of State and Ideal Adsorbed Solution Theory,
529 Langmuir. 35 (2019) 11690–11701.

530 [37] C.M. Simon, B. Smit, M. Haranczyk, pyIAST: Ideal adsorbed solution theory (IAST)
531 Python package, Comput. Phys. Commun. 200 (2016) 364–380.

532 [38] A. Monpezat, S. Topin, L. Deliere, D. Farrusseng, B. Coasne, Evaluation Methods of
533 Adsorbents for Air Purification and Gas Separation at Low Concentration: Case Studies
534 on Xenon and Krypton, Ind. Eng. Chem. Res. 58 (2019) 4560–4571.

535 [39] Y. Li, H. Yi, X. Tang, F. Li, Q. Yuan, Adsorption separation of CO2/CH4 gas mixture on
536 the commercial zeolites at atmospheric pressure, Chem. Eng. J. 229 (2013) 50–56.

537 [40] A.A. Askalany, B.B. Saha, Towards an accurate estimation of the isosteric heat of
538 adsorption–A correlation with the potential theory, J. Colloid Interface Sci. 490 (2017)
539 59–63.

[41] A. Chakraborty, B.B. Saha, S. Koyama, K.C. Ng, On the thermodynamic modeling of the isosteric heat of adsorption and comparison with experiments, Appl. Phys. Lett. 89 (2006) 171901.

[42] A.S. Hyla, H. Fang, S.E. Boulfelfel, G. Muraro, C. Paur, K. Strohmaier, P.I. Ravikovitch, D.S. Sholl, Significant Temperature Dependence of the Isosteric Heats of Adsorption of Gases in Zeolites Demonstrated by Experiments and Molecular Simulations, J. Phys. Chem. C. 123 (2019) 20405–20412.

[43] A.A. Askalany, B.B. Saha, Derivation of isosteric heat of adsorption for non-ideal gases, Int. J. Heat Mass Transf. 89 (2015) 186–192.

[44] L. Valentini, S.B. Bon, O. Monticelli, J.M. Kenny, Deposition of amino-functionalized polyhedral oligomeric silsesquioxanes on graphene oxide sheets immobilized onto an amino-silane modified silicon surface, J. Mater. Chem. 22 (2012) 6213–6217.

[45] M. Peyravi, Synthesis of nitrogen doped activated carbon/polyaniline material for CO2 adsorption, Polym. Adv. Technol. 29 (2018) 319–328. doi:10.1002/pat.4117.

[46] A.M. Shanmugharaj, J.H. Yoon, W.J. Yang, S.H. Ryu, Synthesis, characterization, and surface wettability properties of amine functionalized graphene oxide films with varying amine chain lengths, J. Colloid Interface Sci. 401 (2013) 148–154.

[47] Y. Guo, L. Luo, Y. Zheng, T. Zhu, Optimization of CO2 Adsorption on Solid-Supported Amines and Thermal Regeneration Mode Comparison, ACS Omega. 5 (2020) 9641–9648. doi:10.1021/acsomega.9b03374.

[48] P. Zarabadi-Poor, A. Badiei, B.D. Fahlman, P. Arab, G. Mohammadi Ziarani, One-pot

561 synthesis of ethanolamine-modified mesoporous silica, Ind. Eng. Chem. Res. 50 (2011)
562 10036–10040.

563 [49] S.A.A. Nami, I. Khan, Synthesis and morphological studies of uniquely shaped graphene
564 oxide@ piperazine−polyaniline nanocomposites, Polym. Compos. 38 (2017) E295–E302.

565 [50] S. Loganathan, A.K. Ghoshal, Amine tethered pore-expanded MCM-41: A promising
566 adsorbent for CO2 capture, Chem. Eng. J. 308 (2017) 827–839.

567 [51] V. Zelenak, D. Halamova, L. Gaberova, E. Bloch, P. Llewellyn, Amine-modified SBA-12
568 mesoporous silica for carbon dioxide capture: Effect of amine basicity on sorption
569 properties, Microporous Mesoporous Mater. 116 (2008) 358–364.

570 [52] M.J. McAllister, J.-L. Li, D.H. Adamson, H.C. Schniepp, A.A. Abdala, J. Liu, M.
571 Herrera-Alonso, D.L. Milius, R. Car, R.K. Prud'homme, Single sheet functionalized
572 graphene by oxidation and thermal expansion of graphite, Chem. Mater. 19 (2007) 4396–
573 4404.

574 [53] S. Saxena, T.A. Tyson, E. Negusse, Investigation of the local structure of graphene oxide,
575 J. Phys. Chem. Lett. 1 (2010) 3433–3437.

576 [54] Z.-Y. Sui, Y. Cui, J.-H. Zhu, B.-H. Han, Preparation of three-dimensional graphene
577 oxide–polyethylenimine porous materials as dye and gas adsorbents, ACS Appl. Mater.
578 Interfaces. 5 (2013) 9172–9179.

579 [55] M.R. Mello, D. Phanon, G.Q. Silveira, P.L. Llewellyn, C.M. Ronconi, Amine-modified
580 MCM-41 mesoporous silica for carbon dioxide capture, Microporous Mesoporous Mater.
581 143 (2011) 174–179.

582 [56] G. Yin, Z. Liu, Q. Liu, W. Wu, The role of different properties of activated carbon in CO2
583 adsorption, Chem. Eng. J. 230 (2013) 133–140.

584 [57] X. Li, Y. Ding, L. Guo, Q. Liao, X. Zhu, H. Wang, Non-aqueous energy-efficient
585 absorbents for CO2 capture based on porous silica nanospheres impregnated with amine,
586 Energy. 171 (2019) 109–119.

587 [58] F. Jiang, W. Zhao, Y. Wu, Y. Wu, G. Liu, J. Dong, K. Zhou, A polyethyleneimine-grafted
588 graphene oxide hybrid nanomaterial: Synthesis and anti-corrosion applications, Appl.
589 Surf. Sci. 479 (2019) 963–973.

590 [59] Y. Liu, B. Sajjadi, W.-Y. Chen, R. Chatterjee, Ultrasound-assisted amine functionalized
591 graphene oxide for enhanced CO2 adsorption, Fuel. 247 (2019) 10–18.

592 [60] C. Xue, L. Feng, H. Zhu, R. Huang, E. Wang, X. Du, G. Liu, X. Hao, K. Li, Pyridine-
593 containing ionic liquids lowly loaded in large mesoporous silica and their rapid CO2 gas
594 adsorption at low partial pressure, J. CO2 Util. 34 (2019) 282–292.

595 [61] Y. Zhang, Y. Chi, C. Zhao, Y. Liu, Y. Zhao, L. Jiang, Y. Song, CO2 Adsorption Behavior
596 of Graphite Oxide Modified with Tetraethylenepentamine, J. Chem. Eng. Data. 63 (2017)
597 202–207.

598 [62] G.J. Shin, K.Y. Rhee, S.J. Park, Improvement of CO2 capture by graphite oxide in
599 presence of polyethylenimine, Int. J. Hydrogen Energy. 41 (2016) 14351–14359.
600 doi:10.1016/j.ijhydene.2016.05.162.

601 [63] S.M. Hong, S.H. Kim, K.B. Lee, Adsorption of carbon dioxide on 3-aminopropyl-
602 triethoxysilane modified graphite oxide, Energy and Fuels. 27 (2013) 3358–3363.

603 doi:10.1021/ef400467w.

604 [64] H. Ning, Z. Yang, D. Wang, Z. Meng, Y. Li, X. Ju, C. Wang, Graphene-based semi-coke
605 porous carbon with N-rich hierarchical sandwich-like structure for efficient separation of
606 CO2/N2, Microporous Mesoporous Mater. (2020) 110700.

607 [65] N.F.T. Arifin, N.A.N. Zulkipli, N. Yusof, A.F. Ismail, F. Aziz, W.N. Wan Salleh, J.
608 Jaafar, N.A.H.M. Nordin, N. Sazali, Preparation and characterization of APTES-
609 functionalized graphene oxide for CO2 adsorption, J. Adv. Res. Fluid Mech. Therm. Sci.
610 61 (2019) 297–305.

611 [66] W. Rudzinski, S.-L. Lee, C.-C.S. Yan, T. Panczyk, A fractal approach to adsorption on
612 heterogeneous solid surfaces. 1. The relationship between geometric and energetic surface
613 heterogeneities, J. Phys. Chem. B. 105 (2001) 10847–10856.

614 [67] A. Samanta, A. Zhao, G.K.H. Shimizu, P. Sarkar, R. Gupta, Post-combustion CO2 capture
615 using solid sorbents: a review, Ind. Eng. Chem. Res. 51 (2011) 1438–1463.

616 [68] V.C. Srivastava, I.D. Mall, I.M. Mishra, Adsorption thermodynamics and isosteric heat of
617 adsorption of toxic metal ions onto bagasse fly ash (BFA) and rice husk ash (RHA),
618 Chem. Eng. J. 132 (2007) 267–278.

619 [69] T. Watabe, K. Yogo, Isotherms and isosteric heats of adsorption for CO2 in amine-
620 functionalized mesoporous silicas, Sep. Purif. Technol. 120 (2013) 20–23.

621 [70] R. Sanz, F. Martínez, G. Orcajo, L. Wojtas, D. Briones, Synthesis of a honeycomb-like
622 Cu-based metal–organic framework and its carbon dioxide adsorption behaviour, Dalt.
623 Trans. 42 (2013) 2392–2398.

624